

## Structure and Properties of Co-Cr Coatings After a Pulsed Jet Treatment

**Abstract.** Presents new results on formation and structure of plasma jet, its interaction with working surface regions (in situ). Operation principles of plasma-detonation device (Impulse-6) and application of this technology for Co-Cr coating deposition and tool surface hardening were described. Obtained experimental values of jet parameters (temperature, duration, power), as well as time scanning for current pulses and voltages allowed us to optimize jet parameters for deposition of ceramic, metal-ceramic and alloy coatings to stainless steel substrates. Coating structure was mainly composed of  $\alpha$ -fcc- and  $\beta$ -fcc-cobalt. Selected temperature interval for coating formation, according to XRD analysis, allowed us to form intermetalloid compounds of  $\text{Co}_x\text{Cr}_y$ -type cobalt with chromium.

**Streszczenie.** Zaprezentowano nowe wyniki badań tworzenia i struktury impulsu plazmowego oraz jego interakcji z regionami powierzchni roboczej (in situ). Opisane zostały zasady działania komory detonacyjnej (Impulse-6) i zastosowania tej technologii do nakładania powłok Co-Cr i utwardzania powierzchni narzędzi. Otrzymane wartości eksperymentalne parametrów impulsu plazmowego (temperatura, czas trwania, moc) jak również czas skanowania impulsów prądowych i napięć pozwoliły zoptymalizować parametry impulsu plazmowego do nakładania powłok ceramicznych, metaliczno-ceramicznych i stopowych na podłoża ze stali nierdzewnej. Struktura powłoki była złożona głównie z kobaltu  $\alpha$ -fcc- i  $\beta$ -fcc-. Przedziały temperatur wybrane do tworzenia powłok, zgodnie z analizą XRD, pozwoliły na stworzenie intermetaloidalnych związków kobaltu i chromu typu  $\text{Co}_x\text{Cr}_y$ . (**Budowa i właściwości powłok Co-Cr poddanych obróbce strumieniem impulsów plazmy**).

**Keywords:** melted surface, protective coating, Co-Cr based alloys, wear, hardness, corrosion.

**Słowa kluczowe:** roztopiona powierzchnia, powłoka ochronna, stopy oparte na Co-Cr, zużycie, twardość, korozja.

### Introduction

The use of protective coatings for Improved mechanical and physical-chemical properties of metals and alloys is now an urgent task of materials science. From [1, 2, 4] is well known that coating of PG-19N-01, PG-10N-01, PGAN-33 (based on Ni-Cr and other additives such as Si, B, Fe, W, Mo) used to protect specimens and steel products. This increases the hardness, wear resistance and improves the corrosion resistance after coating with an electron beam melting, or plasma jet. Other authors investigated coverage based on Ni-Al, Al-Co, Al-Mg-Cu,  $\text{Al}_2\text{O}_3$ ,  $\text{Al}_2\text{O}_3 + \text{Cr}_2\text{O}_3$ , WC-Co,  $\text{Cr}_3\text{C}_2$ -Ni, etc. [3 - 5], which also perform protective functions for products made of steels and alloys [4]. The methods for deposition of coatings used detonation, plasma-detonation, a combination of methods, such as detonation and subsequent melting of the surface layer.

To reach high quality of coatings of powder materials with different thermal-physical and thermal-dynamical properties ( $\text{Al}_2\text{O}_3$ ,  $\text{Cr}_2\text{O}_3$ , WC-Co-Cr,  $\text{Cr}_3\text{C}_2$ -NiCr, Al-Ni, Ni-Cr, Co-Cr, etc.) and optimize parameters (development of coating deposition technology), we need direct investigations (measurements) of plasma jet parameters in-situ. For this purpose, two cycles of investigations were performed in this work, which served the basis for optimization of parameters of plasma-detonation device "Impulse-6". Also, the goal of this work was to study the structure and properties of powder materials on Co-Cr base deposited using the high-velocity plasma-detonation jet on (321 stainless steel with Mo) the stainless steel substrate before and after this plasma jet treatment applying also coating surface layer melting.

Purpose of this study was to investigate the structure and physico-chemical properties of coatings produced from a mixture of two powders Ni-Cr-B-Si-Fe/WCo, caused by high-speed plasma jet by using a detonation and plasma-detonation technology.

### Experimental Methods

We formed the protecting coatings of 300 to 500  $\mu\text{m}$  thickness from the powder alloy PGAN-35 on cobalt base with the following composition: Cr (8 to 32%); Ni ( $\leq 3\%$ ); Si (1.7 to 2.5%); Fe ( $\leq 3\%$ ); C (1.3 to 1.7%) and W (4 to 5%) on the substrate of stainless steel 12X18M9 (321 stainless

steel with doped Mo 6-9 at%). Using the plasma-detonation facility "Impulse-6". The powder with fraction dimensions 56 to 200  $\mu\text{m}$  was used. Steel samples of 20x30x2 mm, which surfaces were preliminarily subjected to sand-blasting treatment, were used as the substrate materials. Plasma-detonation powder materials were deposited using the following regimes for pulsed-plasma deposition: a distance from the sample to the plasmatron (detonation gun for deposition) nozzle was 60 mm, a velocity of sample motion was 360 mm/min. frequency of pulsed repetition exceeded 4 Hz, powder expenditure was 21.6 g/min, capacity of a capacity battery was 800  $\mu\text{F}$ , and propane, oxygen and air were used as combustion and plasma-forming gases. We chose Mo for the material of doping electrode. After cooling samples in the plasmatron chamber a half of the samples was covered, and the other half was treated by pulsed plasma flows till melting for one to three passes. Operation regimes of the plasmatron were the same as in the case of deposition, however, the pulsed repetition frequency was 2.5 Hz. After this the samples were spark cut into pieces, studied and subjected to different tests.

The surface morphology was studied using scanning electron microscopy with reflected and secondary electron modes a scanning electron microscope REMMA-103-01, (Selmi, Sumy, Ukraine) and optical profiler VEECO WYKO NT 1100 (AZ 85706 USA) To determine a chemical composition used energy dispersive X-ray spectroscopy (EDS). The surface phase composition was analyzed by X-ray structure analysis using an X-ray diffraction facility DRON-2 (St.-Petersburg, Russia) in  $\text{CuK}\alpha$  emission under conditions of Bregg-Brentano focusing. The diffraction patterns were taken by an continuous X-ray scan in the range of  $2\theta$  angles from  $20^\circ$  to  $100^\circ$ . We interpreted diffraction peaks using a data base PCPDWIN.

Microhardness measurements for plasma-detonation produced powder coatings were performed using a PMT-3 (St.-Petersburg, Russia) apparatus with a diamond Vickers's pyramid under indenter load 10, 25, 50 g. Nanohardness tests were performed by a three-side Berkovich indenter of a nanohardness facility Nano Indenter-II (USA). These tests were performed in the following way: first, loading till 10mN, then hold during 20 sec, then the load was decreased to 80%, stay under a

constant load during 30 sec to measure a heat drift, and finally we applied full indenter loading. To determine hardness and elastic modulus under maximum loading of the indenter, we used methods of Oliver and Pharr [6]. Wear resistance tests were performed using the apparatus SMTs-2 (Kiev, Ukraine) according to the set-up "plane-cylinder" in a medium of technical vaseline. A criterion for evaluation of the samples' friction performance was the material volume ablated in the friction zone. The bulk wear was measured by microweighing every 800 cycles. A total number of rotations (a counter body or an engine) were about 10000. Corrosion resistance tests of a modified coating were performed using a Bank-Wenking Potentiogalvanostat PGS 81R and cells Princeton Applied research corrosion test. The tests were performed in sulphuric acid solution 0.5M under temperature up to 200°. Potential from 1 to 1.3V was applied to the facility electrodes. In all cases the samples surface exposed to the corroding medium was 1 cm<sup>2</sup>. The test in 0.5 M H<sub>2</sub>SO<sub>4</sub> solution were carried out in the potential region – 1000 to + 1500 V at ambient temperature. Five rapid scans (scan rate = 25 mV/s) followed by one slow scan (scan rate = 0.25 mV/s) were performed on specimen.

## Results and Discussion

Figure 1a taken from the optical microscopy, shows that plasma-detonation modification of a stainless steel surface in the case we applied cobalt-based powder coating deposition was accompanied by formation of the strongly alloyed structure. The surface structure of such coatings looked scaly and flaky. These coatings had highly pronounced relief without acute protrusions. Also we in the surface we observed many deformed protuberances, which looked as powder particles in-melted into the surface. First of all, we relate this to wide spread in powder particle dimensions – from 56 to 200 μm. During their flight in the pulsed plasma jet small particles were totally melted, but those of bigger dimensions – only partially and being deformed on impacting formed the coating matrix. A mechanism of powder coating formation was the following:

- The substrate surface treatment by high-energy plasma jet with high ion and electron density (1 to 5) × 10<sup>17</sup> cm<sup>-3</sup> intensified electron heat conductivity and heating of an external substrate material layer.
- Moving with high rate developed in the process of detonation of plasma-forming gases powder particles were melted in the high-temperature plasma jet of pulsed plasma. In a first pass when impacting the substrate they were deformed and filled in various micro-valleys in the substrate surface.

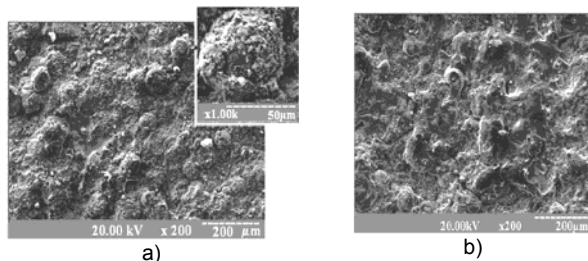


Fig. 1 Surface morphology of plasma-detonation produced coatings of AN-35 powder: a) an initial surface state; b) coatings after HVPJ melting (two passes)

Figure 2 shows images of cross-sections taken from the metallographic microscope for the samples with PGAN-35 coating. These photos show that both the transition region structure and that of the coating had a complicated character. As a result of mechanical and thermal treatment

of a two-phase plasma-detonation flow by dynamical introduction of the powder material into the near surface substrate regions we succeeded to form a desired coating. After the transversal cross-sections were etched, along the contact boundary we found white bands which were not able to be etched, a region of  $h_1$  thickness). Analysis of the coating surface structure demonstrated that it was composed of the regions of entire coating with in-melted powder particles and small in diameter cavities. Photos shown in Fig. 2a also demonstrate that in the process of coating formation the most powder fraction moving with high velocity and getting melted strongly in a high-temperature pulsed plasma jet impacted the surface and when impacting was strongly deformed and spread out.

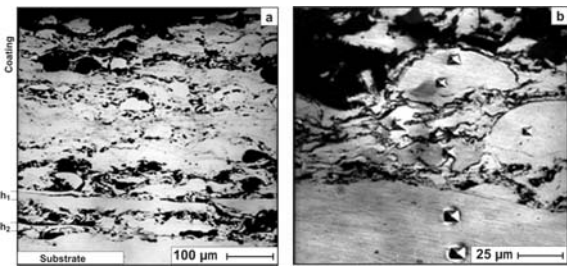


Fig.2. Optical photos of various resolutions taken using a microscope for transversal cross-sections: a) images for coating and substrate structure from the transversal cross-section; b) images for that coating region, which was used to measure microhardness

The powder material filled in various valleys occurring in the substrate surface and powder coating after every subsequent pass. However, moving with high velocity the powder flow was saturated by elements of a plasmatron gas atmosphere, and some weakly melted particles "covered" various valleys conditioning occurrence of pores in the coating structure. The bigger the diameter of a particle, the lower it was heated in a plasma jet and impacting with the substrate surface it formed local regions of strengthened state in the surface, which we considered to be a good sign for forming strong adhesion power. The coating structure itself was such that those powder layers that were positioned closer to the substrate surface had much lower porosity than those of the near surface region. We assumed that probably with increased number of passes the lower positioned layers were hardened due to action of thermal and mechanical loads. Also it is probable that after every subsequent pass of the plasmatron the deposited surface got cooled a little and the following powder layer, which was deposited, partially destructed the surface of the previous sublayer introducing in it powder particles. Metallography studies of detonation-produced coating structures demonstrated that the cobalt-based powder deposition process under chosen regimes was accompanied by the formation of a developed interphase boundary between the coating and substrate. As a result of this interaction some places in the substrate surface layer were deformed (the process of "micro-channeling" of powder particles). At the interphase boundary there are regions in which powder particles were introduced into the melted substrate surface at an initial stage of coating formation. Following the interphase boundary we found a region of a transition layer developing approximately to the coating depth. In the process of deposition his transition layer was subjected to high temperature action and mechanical hardening. To study the structure of such coatings and evaluate their element composition, we applied SEM and took imaged of their surface with secondary electrons. The pictures (Fig.3a) show that in the process of deposition a coating with a highly pronounced relief was produced. The surface of such

coatings was composed of a great number of non-fully melted powder particles. We consider that pictures show round regions ( $\leq 50 \mu\text{m}$  in diameter), which seem to be centers of a hard powder matrix. Our studies of a local and integral element composition (Fig.3b) of the powder coatings demonstrated that their matrixes possessed high

atomic concentration of Co (about 19.17 wt.%) In addition we found about 21wt% of Cr; 30.5wt% of Fe, 3.5wt% of Si and 4.7wt% of Ni, carbon, molybdenum (the material of doping electrode) and calcium playing a role of impurity elements. They only sweated together with other non-uniformities.

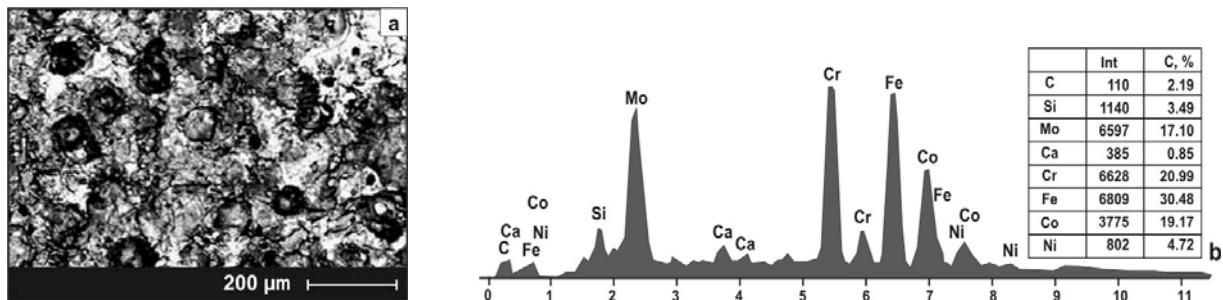


Fig.3. Structure and chemical composition of the plasma-detonation produced coating: a) a photo for the surface region subjected to element analysis (under secondary electron regime conditions); b) integral element surface composition

SEM analysis performed in some regions of the coating demonstrated that the same structure as in the case of concentrated energy flow treatment (CEFT) was formed in the surface. Coating surface morphology studies demonstrated that some changes took place in the coating matrix under selected regimes of surface thermal modification. The obtained photos show that the HVPJ treatment was accompanied by through-melting of the surface since an amount of non-fully melted powder particles decreased essentially in the coating matrix. Traces of some powder particles remained in the photos, but they were significantly lower in diameter, and the coating itself had higher degree of alloying. Surface melting by pulsed plasma flows provided also changed element composition of near surface coating layers. To evaluate parameters of relief roughness for Co-Cr coating surface after plasma jet melting, we additionally employed an optical microscope with laser attachment VEECO. The photos of the near surface region demonstrate many brightly glowing areas of irregular forms (Fig. 4a). Earlier we found that near surface coating regions formed without melting had a porous structure. But in the process of melting an amount and dimensions of these pores essentially decreased, and those which remained were filled-in by atoms of the eroding electrode.

Distribution of basic coating elements over depth at points, which are marked in Fig. 4 are summarized in Table 1. According to obtained result of analyses distribution of the coating composing elements practically does not change from point to point. We assume that presence of molybdenum atoms in powder coatings was due to its presence in the plasmatron gas atmosphere and the result of deposition process, since distribution of molybdenum atoms over the coating depth and width shows uniform character.

Table 1. Distribution of Elements Content over Depth of Powder Coatings after HVPJ Modification

Po-int	Concentration, wt.%								
	C	Si	Mo	Cr	Fe	Co	Ni	W	Mn
1	0.45	1.34	1.00	31.56	1.86	57.35	2.71	2.73	-
2	0.53	0.33	2.64	17.56	66.19	1.08	10.69	-	-
3	0.51	1.33	1.02	30.09	1.74	58.7	3.06	2.56	-
4	-	2.26	1.38	32.32	1.52	57.42	3.48	-	0.61
5	-	2.24	1.21	30.51	1.92	55.87	7.26	-	0.48
6	-	2.51	1.39	31.86	1.59	57.41	3.56	-	0.69
7	0.48	1.13	1.08	30.07	2.82	57.86	3.05	2.5	-
8	0.78	1.12	0.99	29.61	3.17	57.86	3.01	2.45	-
9	0.62	0.98	0.95	30.45	2.45	58.27	2.7	2.55	-
10	-	-	94.33	-	1.34	3.33	-	-	-
11	-	-	97.99	0.30	-	0.71	-	-	-

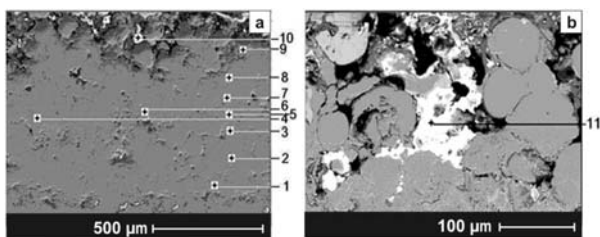


Fig.4. Results of studies for distribution of coating element composition over depth after HVPJ treatment (crosses mark the points of local element analysis): (a) photos for some region of the powder coating cross-section; (b) the structure of powder coating near surface regions after melting (under secondary electron regime conditions)

Figure 4b demonstrates the structure of near surface regions of the resulting coating more clearly. Studies of the surface element composition by micro analysis demonstrated that these light aggregates by 95% are composed of molybdenum atoms. Integral spectra of the coating surface element composition after melting demonstrated high intensity chromium, iron and cobalt peaks.

However, physical and mechanical surface properties are determined not only by its morphology and elements composition. When the coating porosity is low their hardness will be dependent on the surface phase composition. Using X-ray analysis we found that the powder which was used for deposition was composed of a solid solution  $\alpha$ - and  $\beta$ - Co. We assumed that Ni, Si, Fe, Cr and W played a role of substitution atoms. In spite of significantly high chromium content occurring in the powder, its peaks in the diffraction image are absent (Fig. 5a). This means that all the chromium atoms have chemical bonds with those of cobalt. As a result of plasma-detonation coating deposition induced by the pulsed plasma jet an initial powder material underwent a number of phase transformations. Also a solid cobalt solution  $\beta$  (fcc) and  $\alpha$  (hcp) are a part of the coating surface. As one can see in a diffraction pattern (Fig. 5b), after coating deposition the peaks corresponding to X-ray reflection from cobalt lattice planes broadened significantly and became less intensive.

We assume that their broadening was due to atomic regrouping in the initial material induced by high temperatures. According to a phase diagram CoCr, in

addition to a-cobalt a phase  $\text{Co}_{60}\text{Cr}_{40}$  must be formed in the coating. Therefore based on the data of this phase diagram and table data, we relate the background increase in the region of angles 26 from 37 to 42 and from 43 to 47 to the formation of cobalt chemical compounds with chromium near the surface. Calculation of a per cent phase ratio in the coating demonstrated that 65 volume% was occupied by cobalt solution, and the rest was for an intermetallic compound of cobalt with chromium.

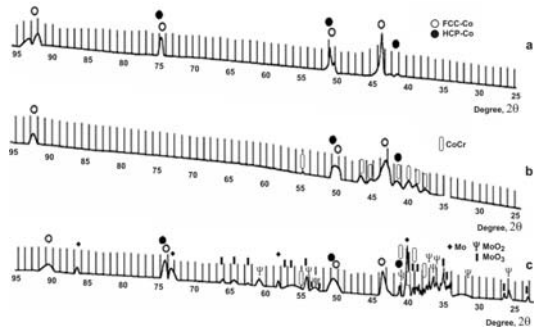


Fig.5. Diffraction patterns fragments taken for: (a) the PGAN-35 initial powder; (b) plasma-detonation powder coatings; (c) the PGAN-35 coatings after subsequent melting by the high-velocity plasma jet

After melting of the coating surface by pulsed plasma jet to the depth till 45 to 60  $\mu\text{m}$  the near surface region also was composed of  $\alpha$ - and  $\beta$ -Co. As for the intermetallic compound  $\text{CoCr}$ , it was at the lowest limit of detection ( $< 5$  volume %). X-ray analysis confirmed that thermal activation of a surface by high-velocity pulsed plasma jet provided saturation of near surface coating layer by molybdenum atoms. The diffraction pattern of Fig. 5c, shows well pronounced intensity peaks corresponding to reflections of (110), (200), and (211) planes for (bcc)-phases of molybdenum. According to the performed calculations the molybdenum lattice parameter was equal to 3.13 ( $a_{\text{bulk}}(\text{Mo}) = 3.147\text{\AA}$ ). Many peaks of low intensity, which we are present in the diffraction patterns attribute to the formation of molybdenum oxide  $\text{MoO}_2$  and  $\text{MoO}_3$  films formed in the coating surfaces in the process of melting. Calculations of a per cent ratio of phases composing the near surface regions of powder coatings demonstrated that matrices are composed by 30 volume % of a solid solution on cobalt base and 20 volume % of molybdenum. The rest 50% are molybdenum oxides and inter metallic compounds of cobalt with chromium. Fig. 6 shows the energy spectra of Rutherford proton back scattering obtained for the sample with PGAN-35 (Co-Cr) coating, whose surface layer was had lean melted by a plasma jet to the depth not less than 40  $\mu\text{m}$ .

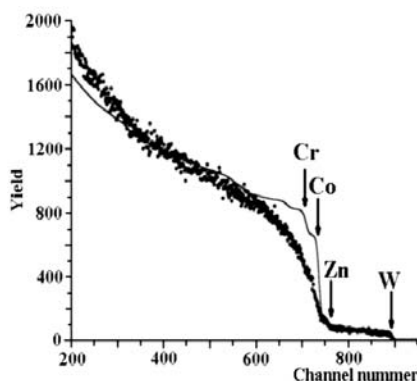


Fig.6. RBS energy spectrum obtained using proton beam  $E_p=2.04$  MeV for stainless steel with coating of PGAN-35 after plasma jet melt ( $\theta=170^\circ$ ,  $\phi=60^\circ$ ). Detector resolution 30keV

Table 2 summarizes the coating composition over its depth, which was obtained from the energy spectra of RBS analysis using a standard program. As one can see from the Figure and Table 2, after melting in the powder coating on Co-Cr base one could find not only 54,72 to 74,16at.% of Co, 14 to 19.67at.% of Cr but also 0.93 to 1.26at.% of W. In addition, in this coating we found about 5at.% of Zn (as a non controlled impurity), which came probably from the plasmatron tube and ignition chamber as a result of plasma jet interaction to their walls. In the sample surface (or in the near surface region) we found an oxygen, the concentration of which reached 25at.% up to 0.3  $\mu\text{m}$  depth.

Table 2. Distribution of Elements Content (RBS) over Depth of Powder Coatings after HVPJ Modification

Depth, nm	Element Concentrations (at %)				
	W	Zn	Co	Cr	O
70.4	0.93	4.90	54.72	14.41	25.04
139.2	0.90	4.90	58.72	14.02	21.46
307.6	0.88	4.90	64.63	13.83	15.76
4902.2	1.26	4.91	74.16	19.67	0.0
15240.1	1.26	4.91	74.16	19.67	0.0

Microhardness measurements performed for HVPJ-produced coatings after their modification, in which we used transversal cross-sections allowed us to obtain the following results:

- the microhardness in the coating near surface region reached  $4.55 \pm 0.35$  GPa;
- its maximum value of  $6.25 \pm 0.34$  GPa was found near the plasma jet melted zone;
- microhardness measurements, which we performed at the half-depth of the coating (120  $\mu\text{m}$ , which corresponded approximately to the interface of melting depth) demonstrated an average value of  $4.20 \pm 0.25$  GPa;
- in a contact region "coating-substrate" an average value of microhardness was about  $3.14 \pm 0.23$  GPa;
- in the process of our studies we also found that an average value of microhardness decreased with increased coating thickness.

In parallel we performed measurements of the produced coating nanohardness. Figure 7 shows curves of loading for the substrate and PGAN-35 coating after melting by a high-velocity pulsed plasma jet. These data evidence that the coating nanohardness is 8.7 GPa and that of the substrate reached 3GPa (the substrate elastic modulus was about 210 GPa).

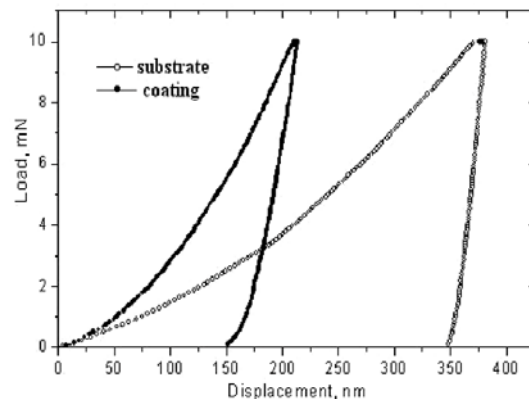


Fig.7. Loading curves taken in substrate nanohardness measurements and the PGAN-35 coating after pulsed plasma flow treatment

Figure 8 shows dependences of wear curves obtained for initial coatings and for those after pulsed plasma modification. From these dependences one can see that the

highest wear was observed in the stainless steel substrate. Plasma detonation deposition of powder coatings decreases substantially the wearing of a treated surface. Thermal coating hardening by pulsed plasma jet allows one to have the most optimum combination of hardness and plasticity. The tests of sample surfaces for wear resistance in technical Vaseline medium demonstrated that:

- deposition of powder coatings on cobalt base under above mentioned regimes resulted in a factor of 12 increase in their surface wear resistance in comparison with substrate material;
- repeated HVPJ treatment of surfaces resulted in a decrease of wear by a factor of 25 (which was likely to be related to Mo oxide formation).

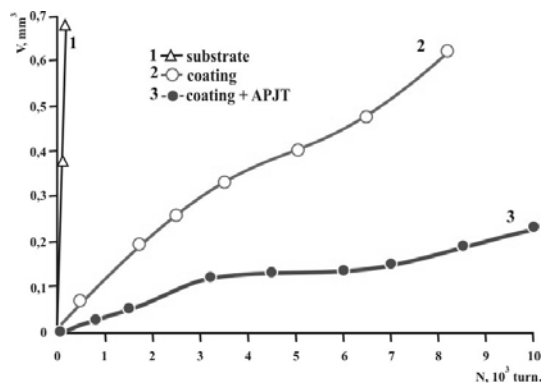


Fig.8. Dependence of surface wear for powder coatings on cobalt base during dry friction on the number of rotations: 1 – the substrate material (stainless steel); 2 – wearing of plasma-detonation produced coatings (240µm thick); 3 – effect of coating surface melting as a result of pulsed plasma flow action (2 passes) on wear resistance

Preliminary tests of ball cocks with such protective coatings under temperature of 200°C in acid medium demonstrated very good corrosion resistance, (17 to 22 times higher than in the substrate).

## Conclusions

Plasma detonation deposition of powder coatings on cobalt base was accompanied by formation of an alloyed powder structure with a highly developed relief. Basic matrix components of these powder coatings were cobalt, chromium, nickel, iron, molybdenum (the eroding electrode element) and carbon (a component of the plasmatron gas atmosphere). In the process of powder deposition in a high-temperature plasma jet the initial material underwent a number of phase transformations after which we found a solid substitution solution of cobalt and intermetallic CoCr compound in the content of produced plasma detonation coatings. In the process of powder deposition we succeeded to develop out of place, a transition region “coating-substrate” with a greatly hardened coating occurring in the vicinity with this zone. Thermal coating modification using a high-velocity plasma jet resulted in a decreased surface relief due to melting of various non-

uniformities and filling-in of valleys in the surface by this liquid material. We also found a decreased porosity of near surface layers by local saturation and simultaneous filling-in of pores by molybdenum atoms.

We conclude that this change in the element and phase composition (appearance of molybdenum oxide films in the surface), the decrease in porosity and surface relief occurred in the process of thermal treatment by high-velocity pulsed plasma treatment resulted in increased nano- and micro-hardness, as well as higher coating wear resistance and their long life in aggressive media.

The authors acknowledge Dr. Ph S.N. Dub (Institute for SuperHard Materials NAS of Ukraine) for their help in performance of these experiments, prof. E.A. Levashov from MISA (Moscow) for their help in performance, prof. A.D. Pogrebnjak (Sumy State University, Ukraine) for help in discussing the results

## REFERENCES

- [1] Misaelides P., Hatzidimitou A., Noli F., Pogrebnjak A.D., Tyurin Yu.N., Kosionidis S., Preparation, characterization, and corrosion behavior of protective coatings on stainless steel deposited by plasma detonation, *Surf. And Coat. Tech.*, 180-181 (2004), 290-296
- [2] Misaelides P., Noli F., Tyurin Y.N., Pogrebnjak A.D., Perdikakis G., Application of ion beam analysis to the characterization of protective coatings prepared by plasma detonation techniques on steel samples, *Nucl. Instr. and Meth. in Phys. Res., Section B.*, 240 (2005), No 1-2, 371-375
- [3] Pogrebnjak A.D., Vasilyuk V.V., Kravchenko Yu.A., Kulmentyeva O.P., Alontseva D.L., Ruzimov Sh.M., Tyurin Yu.N., Bondarev A.A., Duplex treatment of the nickel alloy applied to the steel 3 substrate, *Journal of Friction and Wear*, 25 (2004), No.1, 71-78
- [4] Pogrebnjak A.D., Lebed A.G., Ivanov Yu.F., Modification of single crystal stainless steel structure (Fe-Cr-Ni-Mn) by high-power ion beam, *Vacuum*, 63 (2001), No.4, 483-486
- [5] Pogrebnjak A.D., Bratushka S.N., Il'yashenko M.V., Makhmudov N.A., Kolisnichenko O.V., Tyurin Yu.N., Uglov V.V., Pshik A.V., Kaverin M.V., Tribological and physical-mechanical properties of protective coatings from Ni-Cr-B-Si-Fe/WC-Co-Cr before and after fission with a plasma jet, *Journal of Friction and Wear*, 32 (2011), No. 2, 84-90
- [6] Oliver W.C., Pharr G.M., An improved technique for determining hardness and elastic modulus using load and displacement sensing indentation experiments, *J. Mater. Res.*, 7 (1992), 1564-1583

**Author:** PhD Sergey Bratushka, Sumy State University, 2, R-Korsakov Str., 40007, Sumy, Ukraine, E-mail: s\_bratushka@mail.ru  
 Prof. Marek Opielak, Lublin University of Technology, 38 Nadbystrzycka Str., 20-618 Lublin, Poland  
 Prof. Stefan Liscak, University of Zilina, Faculty of Electrical Engineering, 1 Univerzitna Str., 010 26 Zilina, Slovakia